ACS APPLIED MATERIALS & INTERFACES

Research Article

www.acsami.org

Multifunctional Molecular Design as an Efficient Polymeric Binder for Silicon Anodes in Lithium-Ion Batteries

M. T. Jeena,[†] Jung-In Lee,[‡] Si Hoon Kim,[§] Chanhoon Kim,[‡] Ju-Young Kim,[§] Soojin Park,*[,‡] and Ja-Hyoung Ryu*[,†]

[†]Department of Chemistry, School of Natural Science, [‡]School of Energy and Chemical Engineering, and [§]School of Materials Science and Engineering, Ulsan National Institute of Science and Technology (UNIST), Ulsan, 689-798, South Korea

Supporting Information

ABSTRACT: This work demonstrates the design, synthesis, characterization, and study of the electrochemical performance of a novel binder for silicon (Si) anodes in lithium-ion batteries (LIBs). Polymeric binders with three different functional groups, namely, carboxylic acid (COOH), carboxylate (COO^-), and hydroxyl (OH), in a single polymer backbone have been synthesized and characterized via ^1H NMR and FTIR spectroscopies. A systematic study that involved varying the ratio of the functional groups indicated that a material with an acid-to-alcohol molar ratio of 60:40 showed promise as an efficient binder with an initial columbic efficiency of 89%. This exceptional performance is attributed to the strong adhesion of the binder to the silicon surface and to cross-linking between carboxyl and hydroxyl functional groups, which minimize the disintegration of the Si anode structure during the large volume expansion of the lithiated Si nanoparticle. Polymers with multiple functional groups can serve as practical alternative binders for the Si anodes of LIBs, resulting in higher capacities with less capacity fade.

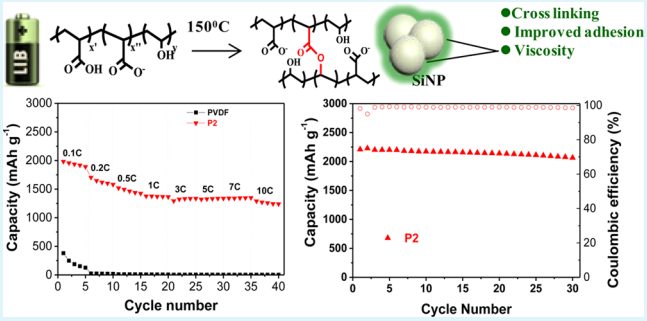

KEYWORDS: *multifunctional binder, polymeric binder, silicon anode, lithium-ion batteries*

INTRODUCTION

Lithium-ion batteries (LIBs) have emerged over the past decade as one of the most promising energy storage and delivery devices because of their high energy densities and high energy efficiencies.[1−4] Among anode materials in development for LIBs, silicon (Si) has great potential because of its high theoretical charge capacity, 4200 mAh g^{-1} for fully lithiated $Li_{22}Si_5$ at high temperature[5−7] or 3579 mAh g^{-1} for metastable $Li_{15}Si_4$ at room temperature.[8−10] These values are almost ten times greater than those of the conventional graphite anode (372 mAh g^{-1}).[11] However, the practical application of Si in LIBs is challenging due to its mechanical fractures and the pulverization of the Si anode resulting from the large volume expansion that the material experiences during lithiation.[12,13] This degree of expansion results in electrically isolated, dead Si particles, rapidly diminishing the capacity of the material for reversible charging. In addition, assuming a Si anode with the maximum insertion capacity of $Li_{22}Si_5$, a volume expansion of the Si corresponds to >300% at this capacity. Si anodes are not fascinating materials when the gravimetric capacity of the Si anode is converted to capacity per unit volume. Structuring of Si particles and developing new polymeric binders are potential strategies to bypass the complications arising from volumetric expansion, thereby maximizing the volumetric capacity of Si-based anode materials.[11] Therefore, many approaches have been put forward by a number of research groups aiming to overcome this issue, including the use of multiphase composites,[14−17] particle size control,[13,18−21] and binder/electrolyte development of Si.[22−26] However, an effective strategy is still on the threshold.

Recent studies have focused on the design of functional polymer binders, which can maximize the contact between anode materials and the current collector and reduce the stress of the Si particles that is induced by the large volume changes experienced during lithiation−delithiation. Several research groups proposed the use of functional-group-enriched binders such as carboxymethyl cellulose (CMC),[27−29] alginate (Alg),[30,31] and poly(acrylic acid) (PAA),[24,32,33] each of which showed better binder performance than the conventional poly(vinylidene fluoride) (PVDF) binders.[34] It was proposed that the chemical interactions between carboxylic acid functional groups of the binders and alcohol functional groups of the surface of Si would be highly beneficial to reduce the disintegration of Si induced by volume expansion.

Though the proper choice of polymeric binder has the potentials to vastly improve the performance of Si anodes, most of the research to date on polymeric binders has been limited to the use of conventional polymer materials or their mixtures.

Received: July 23, 2014
Accepted: September 18, 2014
Published: September 18, 2014

   dx.doi.org/10.1021/am504854x | ACS Appl. Mater. Interfaces 2014, 6, 18001−18007

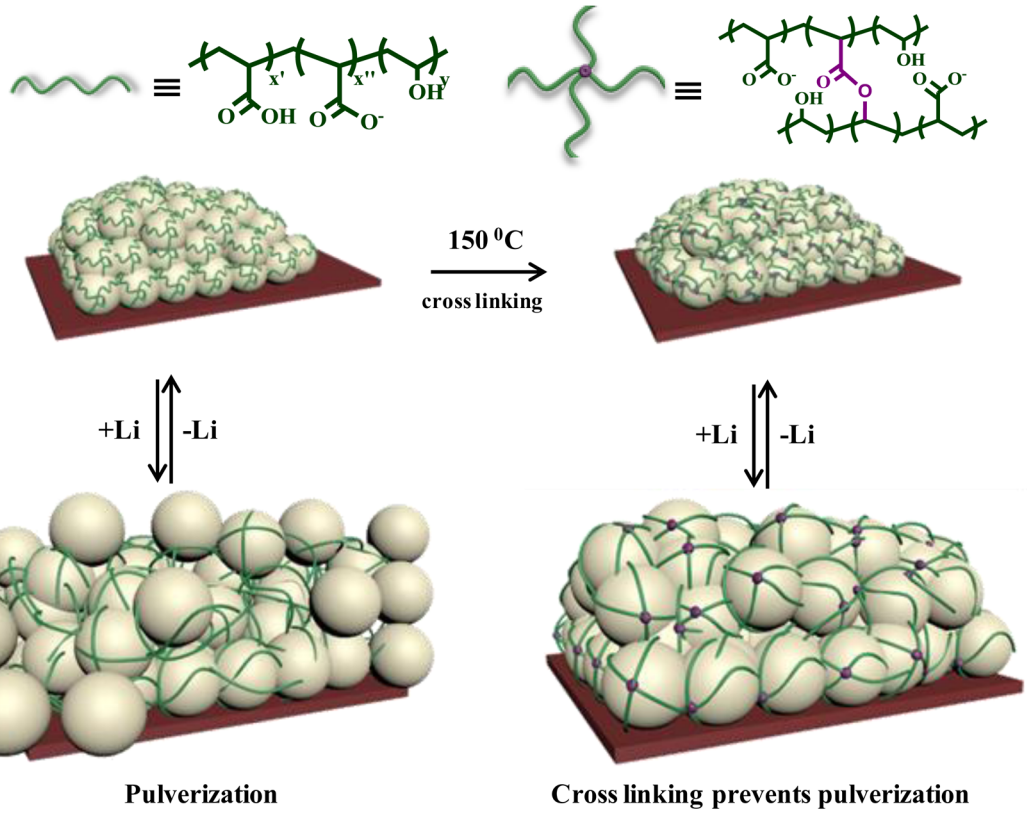

Figure 1. Schematic representation of an efficient binder forming both strong interactions between its acrylate functional groups and silicon nanoparticles and a 3-D intrerconnected network via the condensation of acrylic acid and vinyl alcohol.

Therefore, dedicated synthetic strategies to systemically manipulate the functionality, viscosity, polarity, and flexibility of these materials to enhance their fundamental and systematic understanding are important in any effort to develop an efficient polymer binder for Si anodes.[36] In this paper, we introduce a poly(acrylic acid-*co*-vinyl alcohol) random copolymer as a new binder for the Si anode in LIBs. We have synthesized a series of such random copolymers with varying acrylic acid to vinyl alcohol ratios and investigated the anode performance with each polymeric binder to understand the relationship between molecular structure and electrode performance.

Our molecular design contains three different functional groups in one polymer backbone: acrylic acid, acrylate, and vinyl alcohol (Figure 1). Because each homopolymer studied showed promising electrochemical performance, we hypothesized that the presence of these three different functional groups might act synergistically to provide a more stable and uniform Si anode. Acrylate is a polar functional group that provides a strong interaction between the binder and Si particles and provides good adhesion between the Si anode film and the Cu current collector. The vinyl alcohol functional group is thought to provide high viscosity and flexibility to a binder polymer during water-slurry processing because poly(vinyl alcohol) is a known hydrogels precursor. This allows us to make a uniform anode film with well-distributed active materials. Furthermore, ester formation between carboxylic acid and alcohol might occur during the water drying process at high temperature in vacuo, resulting in a stable electrode film comprising a three-dimensional (3D) interconnected network. Cho et al. reported that PAA/CMC mixture thermally cross-linked to give 3-D networks, which stabilize anode materials and significantly improved the cycle performance of the Si anode by enhancing the mechanical properties of the anode film.[24] Therefore, our specific aim is a systematic investigation to identify an efficient polymeric binder that gives improved adhesion to electrode surfaces, strong interactions between the binder and Si nanoparticles, and optimal mechanical properties through formation of a 3-D film allowing a marked improvement in both capacity and cycle life of the Si anode.

EXPERIMENTAL SECTION

Materials. *t*-Butyl acrylate [stabilized with hydroquinone monomethyl ether (MEHQ), Tokyo Chemical Industries (TCI), Tokyo, Japan] and vinyl acetate [stabilized with hydroquinone (HQ), TCI] were passed through alumina columns before use to remove inhibitors. Trifluoroacetic acid (TFA) (Sigma-Aldrich, Yongin, Korea), silicon nanopowder (average diameter = 100 nm, Alfa Aeser, Ward Hill, MA, USA), potassium carbonate (Samchun Chemicals, Pyeong Teak, Korea), poly(acrylic acid) (PAA) (M_W = ∼100 kDa, Sigma-Aldrich, Yongin, Korea), and poly(vinyl alcohol) (PVA) (Mw = ∼89 kDa, Sigma-Aldrich, Yongin, Korea) were used as received without further purification. Dialysis membranes with molecular weight cut-offs (MWCO) of 12−14 kDa were obtained from Spectra/Pro. Polymers were characterized using 400 MHz FT-NMR spectroscopy, FT-IR spectroscopy, and gel permeation chromatography (GPC) [poly(methyl methacrylate) standard, tetrahydrofuran] (Agilent Technologies, Santa Clara, CA).

Procedure for Synthesis of Poly(acrylic acid-*co*-vinyl alcohol). We used similar procedures to synthesize the random copolymers. For batch **P2**, methyl (ethoxycarbonothioyl)sulfanyl acetate (20 mg, 0.103 mmol) (RAFT reagent), 2,2′-azobis(isobutyronitrile) (AIBN) (5 mg, 0.030 mmol), *t*-butyl acrylate (9.23 mg, 72.10 mmol), and vinyl acetate (8.87 g, 103 mmol) were purged with nitrogen for 15 min in an oven-dried round-bottom flask. The mixture was stirred for 24 h at 65 °C in an oil bath. The resulting

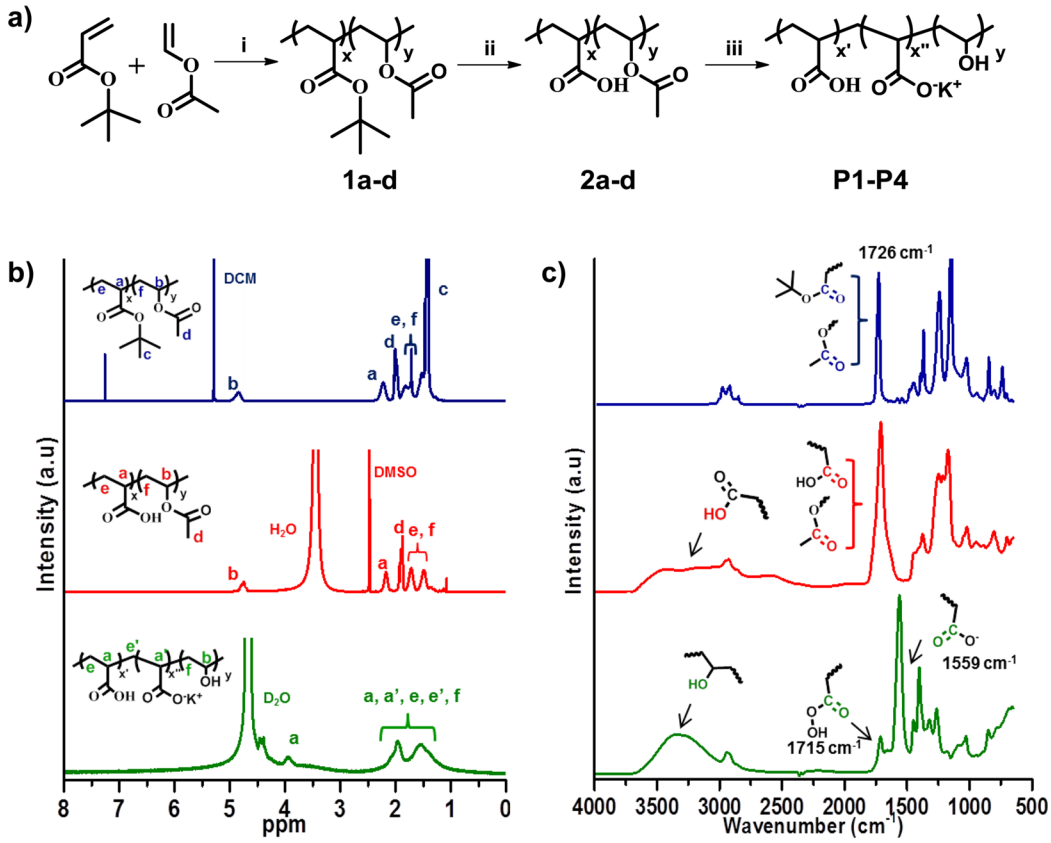

Figure 2. (a) Synthetic approach for the preparation of poly(acrylic acid-*co*-vinyl alcohol), (i) AIBN, RAFT agent, 24 h; (ii) TFA/DCM 24 h; (iii) K_2CO_3/EtOH, 48 h. Characterization of polymers by (b) ^{1}H NMR, and (c) FT-IR.

mixture was precipitated in hexane to obtain the pure product as a white solid (Yield = ~98%). GPC (M_n = 128 kDa, M_w = 360 kDa, dispersity = 2.8). For synthesizing polymers with varying molar ratios, the amount of RAFT agent, AIBN, and vinyl acetate were maintained constant. The amount of *t*-butyl acrylate was varied using the same synthesis procedure as describe above. For synthesizing batches **P1**, **P3**, and **P4**, the amounts of *t*-butyl acrylate used were 3.96 g (30.90 mmol), 13.18 g (103 mmol), and 15.82 g (123.60 mmol), respectively.

Removal of the Protective t-Butyl Group. Poly(*t*-butyl acrylate-*co*-vinyl acetate) (2.00 g) was dissolved in 50 mL of dichloromethane (DCM). TFA (3 mL) was added dropwise to the stirring solution. The reaction mixture was stirred for 24 h at room temperature. Poly(acrylic acid-*co*-vinyl acetate) was precipitated with hexane. The precipitates were washed with DCM and dried under vacuum. The removal of the *t*-butyl group was confirmed by ^{1}H NMR and FT-IR.

Removal of the Protective Acetate Group. Poly(acrylic acid-*co*-vinyl acetate) (1.00 g) was dissolved in ethanol, after which 1.00 g of K_2CO_3 was added to the solution. The reaction mixture was stirred in an oil bath for 2 days at 60 °C. The resulting polymer was precipitated, along with K_2CO_3. The precipitate was collected by filtration. It was then dissolved in water and dialyzed against water with a MWCO 14 kDa dialysis membrane. The final solid polymer was obtained by freeze-drying. The complete removal of the protective acetate group was confirmed by ^{1}H NMR and FT-IR.

Electrochemical Measurements. To test the silicon anode, we used a fabricated coin-type half cell (CR2016 type) composed of a Si working electrode and a metallic lithium counter electrode. The Si electrode contained Si nanoparticles (Alfa Aesar, Ward Hill, MA, diameter ~100 nm, 60 wt %), Super P conductive carbon black (Timcal, Switzerland, 20 wt %), and a polymeric binder (20 wt %). Celgard (Charlotte, NC; Ochang, Korea) 2400 polypropylene microporous membranes were used as separators. The employed electrolyte was composed of 1.3 M $LiPF_6$ in ethylene carbonate/diethylene carbonate (Panaxetech, EC/DEC, 30:70 vol %) with 10 wt % fluoroethylene carbonate (FEC) as an additive. Galvanostatic charge−discharge tests were performed using a cycle tester (WonATech Co., Ltd., Seoul, South Korea) between 0.01 and 1.2 V at room temperature (25 °C).

Nanoindentation Measurement. Nanoindentation experiments were conducted at room temperature using a G200 XP module (Agilent Technologies, Santa Clara, CA) instrument with a three-sided pyramidal Berkovich indenter. Twenty tests were conducted on each sample, to obtain statistically significant data sets. The maximum indentation depths were set at 700 nm, which was less than 1/10 of the sample thickness. While the continuous stiffness measurement (CSM) data do not show stable trends at very shallow indentation depths, primarily because of intrinsic issues in the nanoindentation analysis, the data collected at indentation depths greater than 100 nm show stable trends that are nearly constant for both the hardness and elastic modulus.

RESULT AND DISCUSSION

We synthesized poly(*t*-butyl acrylate-*co*-vinyl acetate) with different molar ratios of the constitutive monomers (Figure 2a). The molar ratios and molecular weights of the polymers were determined from polymers **1a−d**, which still contained only protected functional groups, as the poor solubility of the final polymers in organic solvents led to problems with analyses (Table 1).

The polymers were hydrolyzed to yield **P1−P4** and characterized by FT-IR and ^{1}H NMR during each step of the synthesis. Further details of the syntheses and characterizations of the random copolymers are described in the Supporting Information (see Figure S1−S9).

As shown in Figure 2b, TFA-treatment of polymer **1b** resulted in the disappearance of the *t*-butyl peak at

Table 1. Characterization of Random Copolymer (P1−P4)

polymer	PAA:PVA[i]	Mn (kDa)	PDI[ii]
P1	33:67	75	1.6
P2	60:40	128	2.8
P3	71:29	144	2.2
P4	75:25	150	2.4

[i]The molar ratios were determined by comparing the peak-integrals of the hydrogen attached to the tertiary carbons of tertiary butyl acrylate and vinyl acetate portions of the compound. [ii]Data based on GPC (THF, PMMA standard).

approximately 1.54 ppm in ^{1}H NMR spectrum, indicating the complete deprotection of the *t*-butyl group. Subsequent base hydrolysis of the acetyl group resulted in the desired polymers, as confirmed by FT-IR. Figure 2c shows the shift of the C═O stretching mode of the ester functional groups (top) at approximately 1726 cm^{-1} to 1715 cm^{-1}, which corresponds to the C═O stretching mode of a carboxylic acid (middle). Upon complete hydrolysis, the peak at 1715 cm^{-1} was decreased in conjunction with the appearance of a new intense peak at 1559 cm^{-1}, corresponding to the C═O stretching mode of a carboxylate group (bottom). This indicates the copresence of carboxylic acid and carboxylate, as further confirmed by acidification of the polymer with HCl, which caused the carboxylic acid strech (1715 cm^{-1}) to grow at the expense of carboxylate peak (1559 cm^{-1}) (Supporting Information Figure S10). From the ratios of the peak areas, polymers **P1−P4** were calculated to contain 10−15% carboxylic acid and 85−90% carboxylate. In addition, the increase in intensity of a broad peak located at approximately 3000−3700 cm^{-1} indicates strong hydrogen bonding between the hydroxyl groups produced by the deprotection of vinyl acetate. These results demonstrated that the hydrolysis was complete and that the final polymers contained vinyl alcohol, acrylate, and acrylic acid functionalities.

The effects of the synthetic binders on the electrochemical performance of Si anodes were investigated by galvanostatic measurements. Figure 3a shows the first cycle voltage profiles obtained at 0.05 C between 0.01 and 1.2 V (versus Li/Li$^+$). The random copolymer **P2** exhibited a high specific capacity (2153 mAh g^{-1}) and an excellent initial Coulombic efficiency (ICE) of 89%. These values are comparatively better than those of PVDF (specific capacity = 927 mAh g^{-1}, ICE = 46%), PAA (2000 mAh g^{-1}, 79%), PVA (2133 mAh g^{-1}, 81%), and PAA/PVA binder (2133 mAh g^{-1}, 77%). The superior electro-

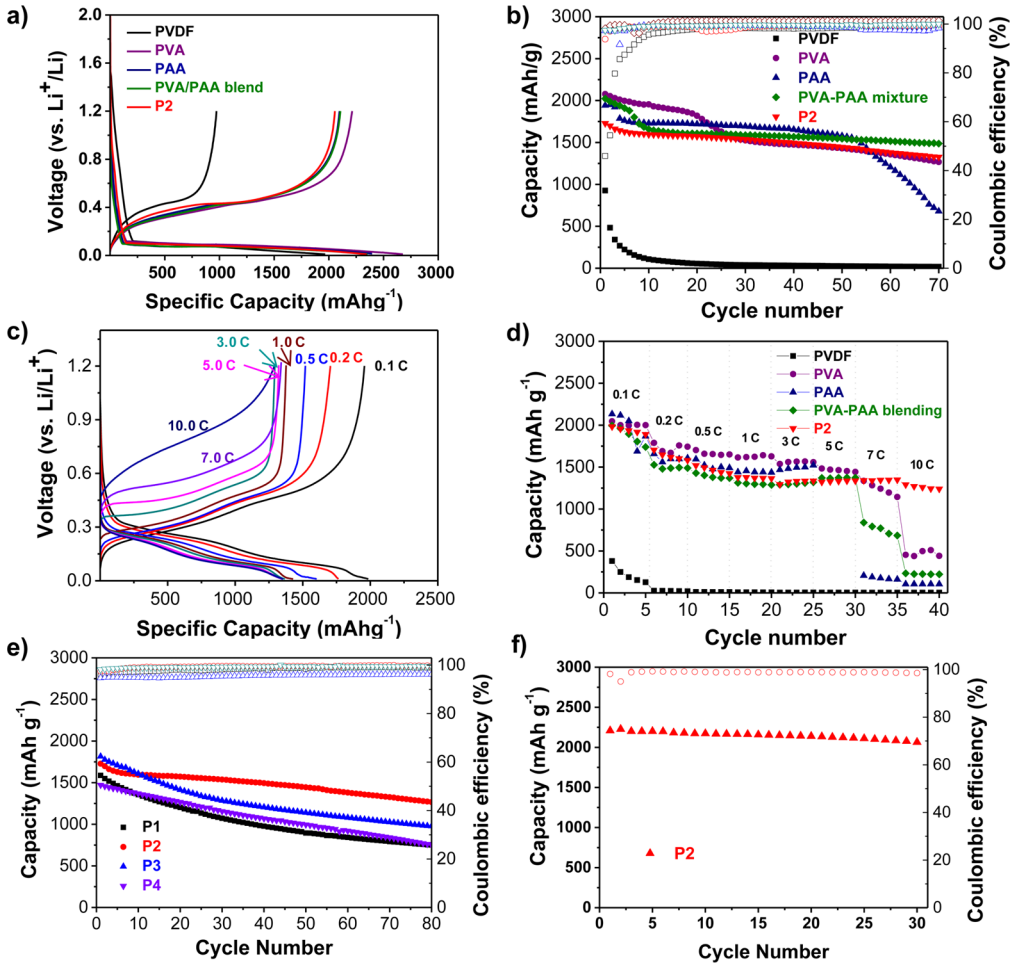

Figure 3. (a) First lithiation/delithiation profile of the Si anode with **P2** in comparison to electrodes containing PAA, PVA, PAA/PVA blend, PVDF (1 C = 2000 mA g^{-1}). (b) Cycling performance profile at a current rate of 0.1 C. (c) Rate performance profile of the Si anode with **P2** at different delithiation C rates ranging from 0.1 to 10 C and a fixed (0.2 C) lithiation C rate. (d) Rate performance of **P2** in comparison to PVDF, PAA, PVA, and PAA/PVA blend. (e) Cycling performance profile of **P2** in comparison to **P1**, **P3**, and **P4**. (f) Specific capacity of **P2** with high mass loading (3 mAh cm^{-2}).

chemical performance of the random copolymer was much more noticeable during cycling. The Si electrode containing the **P2** binder showed the best capacity retention behavior during cycling at a rate of 0.1 C (Figure 3b). PVDF is a poor binder for the Si anode because of the very weak interactions between binder and Si nanoparticles, leading to the desquamation of active materials from the current collector during cycling.

PAA and PVA showed moderate performance due to the surface adhesion promoted by their functional groups, and the strong hydrogen bonding interactions that the materials form with the SiO_2 surface of Si nanoparticles. However, these binders showed decreasing capacities when the cycling was increased, indicating that their binding properties are suboptimal. Moreover, we investigated the rate capabilities of the Si electrodes containing the **P2** binder (Figure 3c), and found that the cell was capable of sustainable cycling at 0.1, 0.2, 0.5, 1, 3, 5, and 10 C with delithiation capacities of 1956, 1704, 1519, 1377, 1350, 1340, and 1291 mAh g^{-1}, respectively. The delithiation capacities at current rates of 5 and 10 C were 78% and 76% of the value at 0.2 C. The rate capabilities of the Si electrode containing **P2** are far superior to those of Si electrodes with other binders (Figure 3d), indicating that the inclusion of **P2** in the electrode contributes to improvement of the rate capability as a result of the interconnected network that the material forms with Si.

To investigate the effect of the ratio between acrylic acid and vinyl alcohol in the polymeric binder, we performed galvanostatic measurements on **P1**−**P4**. Among the four polymers, **P2** (60:40 ratio) showed the best electrochemical performance (Figure 3e). When the fraction of acrylic acid is increased in the random copolymer (**P3** and **P4**), the material takes on properties resembling those of PAA, which embrittles the electrode and leads to deceasing capacity during cycling. This finding shows that decreasing the amount of PAA may weaken the interactions between the Si particles and the binder polymer. Therefore, we conclude that the balance of each functional group plays a vital role in enhancing the electrochemical performance of Si particles through a combination of increasing adhesion properties, forming strong interactions with Si particles, and allowing the material the flexibility to withstand the mechanical stresses induced by the volume changes of the Si particles. Moreover, we tested cycle retention with a high mass loading (3 mAh cm^{-2}) using **P2** binder to investigate the potential for practical LIBs. **P2** binder showed a highly stable charge capacity (2000 mAh g^{-1}) over 30 cycles with a high coulombic efficiency (>99%) (Figure 3f). This result indicates that the cross-linked networks constructed of flexible vinyl alcohol units may inhibit cracking of the anode film under mechanical stress during severe volume expansion/contraction.

The superior cycling performance of the random copolymer binder may be explained by various synergistic advantages originating from its smart molecular design. First, the viscosity of the aqueous polymer−binder solution plays an important role in determining electrode performance. The aqueous solution of random copolymer showed a much higher viscosity and sticky nature compared with a PAA aqueous solution, because of the presence of the vinyl functional groups (Supporting Information Figure S12). This viscous nature enabled the formation of a uniform slurry with active materials and enhances the even distribution of the casting film on the current collector.[35] The high viscosity prevents sedimentation and aggregation of the Si particles during the electrode synthesis, resulting in the formation of a highly uniform film after water evaporation. Second, the softness of anode film can accommodate the large volume changes that occur during the lithiation/delithiation process. While the PAA polymer is glassy to make crake during cycling, which is observable in Figure 3b as the sudden drop in specific capacity after 55 cycles, vinyl alcohol in the random copolymer can reduce the glass nature of the PAA, increasing flexibility. Finally, inter- or intramolecular condensation reactions between the carboxylic acid moieties and hydroxyl groups act to form a stable three-dimensional network. This reaction can be accelerated during the drying process by high temperatures (150 °C) under vacuum conditions. The cross-linked structure limits the deformation of the composite electrode, leading to long-term cycling stability in LIBs. The presence of this highly interconnected network was clearly confirmed by FT-IR spectroscopy. As shown in Figure 4a, the thermally treated film showed a shift of the carboxylic acid C═O stretch at 1715 cm^{-1} toward 1760 cm^{-1}, which corresponds to the C═O stretching in a carboxylate ester. This indicates that most of the carboxylic acid is transformed into the ester functional group. Thermal treatment of PAA under vacuum resulted in the emergence of a

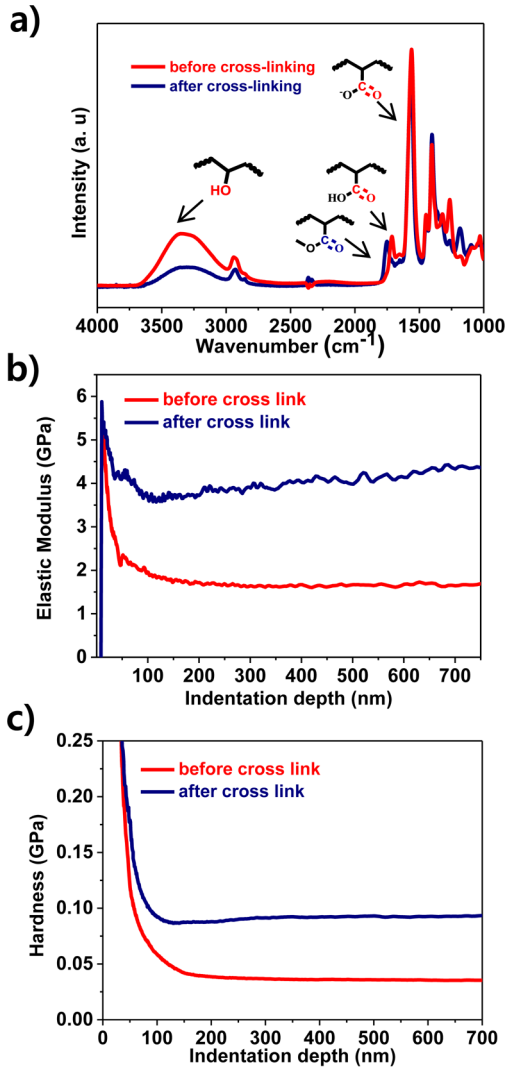

Figure 4. (a) FTIR spectra of **P2** before and after cross-linking. (b) Elastic modulus and (c) hardness of **P2** before and after cross-linking, as measured by nanoindentation.

distinct peak at 1800 cm^{-1} due to the formation of anhydride[24] (Supporting Information Figure S11); the absence of this peak in the copolymer indicates that the cross-linking in the PAA-*co*-PVA binder is ester-type, rather than anhydride. The considerable decrease in the intensity of the peak at 3300 cm^{-1}, indicative of the −OH stretching mode of an alcohol, further confirmed irreversible ester formation between the carboxylic acid and vinyl alcohol. The remaining hydroxyl groups may improve adhesion with the surfaces of the Si nanoparticles or current collector and may provide the anode with a degree of softness, thereby enabling reversible deformation during cycling.

To confirm the robustness of PAA-*co*-PVA random copolymer binder as a mechanical and electrical support, lithium rate capacities using the copolymer binder were compared with capacities with homopolymer binders. While PAA, PVA, and PAA/PVA binders showed considerable capacity-fading at a very high current density (30 A g^{-1}), corresponding to 10 C rate, the **P2** binder retained high lithium extraction capacities (∼1300 mAh g^{-1}) (Figure 3d). This indicates that 3D interconnected network provides the mechanical properties needed to stably hold the Si nanoparticle in contact with the current collector, while minimizing the deformation of electrode film produced during cycling. Further confirmation of the improved mechanical properties enabled by the 3D network was provided by nanoindentaion experiment with the bare and thermally cross-linked **P2** binder (Figure 4b,c). The **P2** binder showed hardness and elastic modulus values of 0.03 (±0.01) and 1.50 (±0.20) GPa, respectively, before cross-linking. After thermal cross-linking, the **P2** binders exhibited significantly enhanced hardness and elastic modulus value of 0.09 (±0.01) and 3.80 (±0.20) GPa, respectively. This is a result of the three-dimensional interconnected network formed through the thermal condensation of the hydroxyl groups in vinyl functionality and carboxylic acid in acrylic acid functionality, which is consistent with FTIR experiments. Interestingly, the PAA binder showed higher hardness (∼0.24 GPa) and elastic modulus (∼6.5 GPa) than the cross-liked **P2** binder, though the **P2** binders exhibited significantly enhanced electrochemical behavior (Supporting Information Figure S13). Apparently, PAA is too hard to endure the mechanical stress produced by the repeated volume change of the Si nanoparticles during charging and discharging. An efficient binder should have enough hardness, yet sufficient flexibility, to maintain the electrochemical activity.

CONCLUSION

In conclusion, we have introduced poly(acrylic acid-*co*-vinyl alcohol) copolymer binders with a range of functional groups for use with Si anodes in lithium-ion batteries. We have shown that a polymer with PAA:PVA ratio 0.6:0.4, the **P2** polymer binder, exhibits superior performance compared to other binders, including conventional polymers, PVA, PAA, and a PAA/PVA mixture. The strong interaction of the polymer binder with the Si nanoparticle present with PAA, along with the high viscosity from PVA, result in a synergetic effect useful for the formation of a uniform anode film. Furthermore, three-dimensionally interconnected networks provide mechanical properties which circumvent the destruction of the electrode during repeated cycling. Taken together, these results demonstrate that the systematic molecular design of novel binder is one of the best strategies for the production of materials that ensure a high charge capacity in LIBs by preserving electrode integrity while maintaining electrical contact during expansion/contraction of silicon anode.

ASSOCIATED CONTENT

Supporting Information

Experimental sections, NMR, GPC, FT-IR spectra of PAA/PVA binders. Viscosities and mechanical properties of polymers. Electrochemical behaviors of Si electrode with polymer binders. This material is available free of charge via the Internet at http://pubs.acs.org.

AUTHOR INFORMATION

Corresponding Authors

*E-mail: spark@unist.ac.kr.
*E-mail: jhryu@unist.ac.kr.

Author Contributions

M. T. Jeena and Jung-In Lee contributed equally to this work. The manuscript was written with contributions from all authors. All authors have given approval to the final version of the manuscript.

Notes

The authors declare no competing financial interest.

ACKNOWLEDGMENTS

This work was supported by a National Research Foundation of Korea (NRF) grant funded by the Korean Government (Ministry of Education, Science and Technology, NRF-2011-35B-C00024), the BK21 Plus funded by the Ministry of Education (10Z20130011057), and Ulsan National Institute of Science and Technology (2013 Future Challenge Research Fund, 1.130038).

REFERENCES

(1) Zheng, F.; Zhu, D.; Chen, Q. Facile Fabrication of Porous NixCo3−xO4 Nanosheets with Enhanced Electrochemical Performance As Anode Materials for Li-Ion Batteries. *ACS Appl. Mater. Interfaces* **2014**, *6*, 9256−9264.
(2) Bhandavat, R.; Singh, G. Improved Electrochemical Capacity of Precursor-Derived Si(B)CN Carbon Nanotube Composite as Li-Ion Battery Anode. *ACS Appl. Mater. Interfaces* **2012**, *4*, 5092−5097.
(3) Lee, J. I.; Lee, E. H.; Park, J. H.; Park, S.; Lee, S. Y. Ultrahigh-Energy-Density Lithium-Ion Batteries Based on a High-Capacity Anode and a High-Voltage Cathode with an Electroconductive Nanoparticle Shell. *Adv. Energy Mater.* **2014**, *4*, 1301542.
(4) Goodenough, J. B.; Kim, Y. Challenges for Rechargeable Li Batteries. *Chem. Mater.* **2010**, *22*, 587−603.
(5) He, Y.; Yu, X.; Wang, Y.; Li, H.; Huang, X. Alumina-Coated Patterned Amorphous Silicon as the Anode for a Lithium-Ion Battery with High Coulombic Efficiency. *Adv. Mater.* **2011**, *23*, 4938−4941.
(6) Wen, C. J.; Huggins, R. A. Chemical Diffusion in Intermediate Phases in the Lithium-Silicon System. *J. Solid State Chem.* **1981**, *37*, 271−278.
(7) Okamoto, H. The Li-Si (Lithium-Silicon) system. *J. Phase Equilib.* **1990**, *11*, 306−312.
(8) Beattie, S. D.; Larcher, D.; Morcrette, M.; Simon, B.; Tarascon, J. M. Si Electrodes for Li-Ion Batteries−A New Way to Look at an Old Problem. *J. Electrochem. Soc.* **2008**, *155*, A158−A163.
(9) Chevrier, V. L.; Dahn, J. R. First Principles Model of Amorphous Silicon Lithiation. *J. Electrochem. Soc.* **2009**, *156*, A454−A458.
(10) Key, B.; Bhattacharyya, R.; Morcrette, M.; Seznéc, V.; Tarascon, J. M.; Grey, C. P. Real-time NMR Investigations of Structural Changes in Silicon Electrodes for Lithium-ion Batteries. *J. Am. Chem. Soc.* **2009**, *131*, 9239−9249.

(11) Kasavajjula, U.; Wang, C.; Appleby, A. J. Nano and Bulk Silicon Based Insertion Anodes for Lithium-Ion Secondary Cells. *J. Power Sources* **2007**, *163*, 1003−1039.
(12) Beaulieu, L. Y.; Eberman, K. W.; Turner, R. L.; Krause, L. J.; Dahn, J. R. Colossal Reversible Volume Changes in Lithium Alloys. *J. Electrochem Solid-State Lett.* **2001**, *4*, A137−A140.
(13) Chan, C. K.; Peng, H.; Liu, G.; Mcilwrath, K.; Zhang, X. F.; Huggins, R. A.; Cui, Y. High-Performance Lithium Battery Anodes Using Silicon Nanowires. *Nat. Nanotechnol.* **2008**, *3*, 31−35.
(14) Lee, J. I.; Choi, N. S.; Park, S. Highly Stable Si-based Multicomponent Anodes for Practical use in Lithium-Ion Batteries. *Energy Environ. Sci.* **2012**, *5*, 7878−7882.
(15) Lim, K. W.; Lee, J. I.; Yang, J.; Kim, Y. K.; Jeong, H. Y.; Park, S. Catalyst-Free Synthesis of Si-SiOx Core-Shell Nanowire Anodes for High-Rate and High-Capacity Lithium-Ion Batteries. *ACS Appl. Mater. Interfaces* **2014**, *6*, 6340−6345.
(16) Cui, L. F.; Ruffo, R.; Chan, C. K.; Peng, H.; Cui, Y. Crystalline-Amorphous Core−Shell Silicon Nanowires for High Capacity and High Current Battery Electrodes. *Nano Lett.* **2008**, *9*, 491−495.
(17) Johnson, D. C.; Mosby, J. M.; Riha, S. C.; Prieto, A. L. Synthesis of Copper Silicide Nanocrystallites Embedded in Silicon Nanowires for Enhanced Transport Properties. *J. Mater. Chem.* **2010**, *20*, 1993−1998.
(18) Kim, H.; Han, B.; Choo, J.; Cho, J. Three-Dimensional Porous Silicon Particles for Use in High-Performance Lithium Secondary Batteries. *Angew. Chem., Int. Ed.* **2008**, *47*, 10151−10154.
(19) Kim, H.; Seo, M.; Park, M. H.; Cho, J. A Critical Size of Silicon Nano-Anodes for Lithium Rechargeable Batteries. *Angew. Chem., Int. Ed.* **2010**, *49*, 2146−2149.
(20) Park, M. H.; Kim, M. G.; Joo, J.; Kim, K.; Kim, J.; Ahn, S.; Cui, Y.; Cho, J. Silicon Nanotube Battery Anodes. *Nano Lett.* **2009**, *9*, 3844−3847.
(21) Magasinski, A.; Dixon, P.; Hertzberg, B.; Kvit, A.; Ayala, J.; Yushin, G. High-Performance Lithium-Ion Anodes Using a Hierarchical Bottom-Up Approach. *Nat. Mater.* **2010**, *9*, 353−358.
(22) Choi, N. S.; Yew, K. H.; Lee, K. Y.; Sung, M.; Kim, H.; Kim, S. S. Effect of Fluoroethylene Carbonate Additive on Interfacial Properties of Silicon Thin-film Electrode. *J. Power Sources* **2006**, *161*, 1254−1259.
(23) Chen, L.; Xie, X.; Xie, J.; Wang, K.; Yang, J. Binder Effect on Cycling Performance of Silicon/Carbon Composite Anodes for Lithium Ion Batteries. *J. Appl. Electrochem.* **2006**, *36*, 1099−1104.
(24) Koo, B.; Kim, H.; Cho, Y.; Lee, K. T.; Choi, N. S.; Cho, J. A Highly Cross-Linked Polymeric Binder for High-Performance Silicon Negative Electrodes in Lithium Ion Batteries. *Angew. Chem., Int. Ed.* **2012**, *51*, 8762−8767.
(25) BuddieáMullins, C. High Performance Silicon Nanoparticle Anode in Fluoroethylene Carbonate-Based Electrolyte for Li-ion Batteries. *Chem. Commun.* **2012**, *48*, 7268−7270.
(26) Cui, L. F.; Hu, L.; Wu, H.; Choi, J. W.; Cui, Y. Inorganic Glue Enabling High Performance of Silicon Particles as Lithium Ion Battery Anode. *J. Electrochem. Soc.* **2011**, *158*, A592−A596.
(27) Li, J.; Lewis, R. Dahn. Sodium Carboxymethyl Cellulose, A Potential Binder for Si Negative Electrodes for Li-Ion Batteries. *J. Electrochem. Solid-State Lett.* **2007**, *10*, A17−A20.
(28) Lestriez, B.; Bahri, S.; Sandu, I.; Roué, L.; Guyomard, D. On the Binding Mechanism of CMC in Si Negative Electrodes for Li-ion Batteries. *Electrochem. Commun.* **2007**, *9*, 2801−2806.
(29) Guo, J.; Wang, C. A Polymer Scaffold Binder Structure for High Capacity Silicon Anode of Lithium-Ion Battery. *Chem. Commun.* **2010**, *46*, 1428−1430.
(30) Chockla, A. M.; Bogart, T. D.; Hessel, C. M.; Klavetter, K. C.; Mullins, C. B.; Korgel, B. A. Influences of Gold, Binder and Electrolyte on Silicon Nanowire Performance in Li-Ion Batteries. *J. Phys. Chem. C* **2012**, *116*, 18079−18086.
(31) Ge, M.; Rong, J.; Fang, X.; Zhou, C. Porous Doped Silicon Nanowires for Lithium Ion Battery Anode with Long Cycle Life. *Nano Lett.* **2012**, *12*, 2318−2323.
(32) Magasinski, A.; Zdyrko, B.; Kovalenko, I.; Hertzberg, B.; Burtovyy, R.; C. Huebner, F.; Fuller, T. F.; Luzinov, I.; Yushin, G. Toward Efficient Binders for Li-Ion Battery Si-Based Anodes: Polyacrylic Acid. *ACS Appl. Mater. Interfaces* **2010**, *2*, 3004−3010.
(33) Komaba, S.; Shimomura, K.; Yabuuchi, N.; Ozeki, T.; Yui, H.; Konno, K. Study on Polymer Binders for High-Capacity SiO Negative Electrode of Li-Ion Batteries. *J. Phys. Chem. C* **2011**, *115*, 13487−13495.
(34) Buqa, H.; Holzapfel, M.; Krumeich, F.; Veit, C.; Novak, P. Study of Styrene Butadiene Rubber and Sodium Methyl Cellulose as Binder for Negative Electrodes in Lithium-ion B atteries. *J. Power Sources* **2006**, *161*, 617−622.
(35) Kovalenko, I.; Zdyrko, B.; Magasinski, A.; Hertzberg, B.; Milicev, Z.; Burtovyy, R.; Luzinov, I.; Yushin, G. A Major Constituent of Brown Algae for Use in High-Capacity Li-Ion Batteries. *Science* **2011**, *334*, 75−79.
(36) Jeong, Y. K.; Kwon, T. W.; Lee, I.; Kim, T. S.; Coskun, A.; Choi, J. W. Hyperbranched β-Cyclodextrin Polymer as an Effective Multidimensional Binder for Silicon Anodes in Lithium Rechargeable Batteries. *Nano Lett.* **2014**, *14*, 864−870.